HAL
open science

N,N'-Di-p-tolylformamidinato-bridged mixed-valence iridium(I)-iridium(III) dimers containing a metal-metal dative bond. Synthesis, molecular structure and physicochemical properties

F. Albert Cotton, Rinaldo Poli

To cite this version:

F. Albert Cotton, Rinaldo Poli. N,N'-Di-p-tolylformamidinato-bridged mixed-valence iridium(I)-iridium(III) dimers containing a metal-metal dative bond. Synthesis, molecular structure and physicochemical properties. Inorganic Chemistry, 1987, 26 (4), pp.590-595. 10.1021/ic00251a020 . hal-03545090

HAL Id: hal-03545090

https://hal.science/hal-03545090

Submitted on 27 Jan 2022

HAL is a multi-disciplinary open access archive for the deposit and dissemination of scientific research documents, whether they are published or not. The documents may come from teaching and research institutions in France or abroad, or from public or private research centers.

L'archive ouverte pluridisciplinaire **HAL**, est destinée au dépôt et à la diffusion de documents scientifiques de niveau recherche, publiés ou non, émanant des établissements d'enseignement et de recherche français ou étrangers, des laboratoires publics ou privés.

Contribution from the Department of Chemistry and Laboratory for Molecular Structure and Bonding, Texas A&M University, College Station, Texas 77843

N,N'-Di-*p*-tolylformamidinato-Bridged Mixed-Valence Iridium(I)–Iridium(III) Dimers Containing a Metal–Metal Dative Bond. Synthesis, Molecular Structure, and Physicochemical Properties

F. Albert Cotton* and Rinaldo Poli

Received September 2, 1986

The reaction between $[Ir(\mu\text{-form})(COD)]_2$ (form = *N,N'*-di-*p*-tolylformamidinato ion; COD = 1,5-cyclooctadiene) and 2 equiv of $AgOCOCF_3$ produces $(COD)Ir(\mu\text{-form})_2Ir(OCOCF_3)_2(H_2O)$ (**1**), containing an unprecedented Ir(I)→Ir(III) dative bond. It also contains two monodentate trifluoroacetate groups coordinated to the Ir(III) atom. The compound has been characterized by IR and ^1H, $^{13}C\{^1H\}$, and $^{13}C\{APT\}$ NMR spectra (APT = attached proton test) and by elemental analyses. Interaction between **1** and a number of donor ligands has been investigated by ^1H NMR spectroscopy; the donor ligand replaces the H_2O molecule to afford similar mixed-valence compounds. The compound containing pyridine, $(COD)Ir(\mu\text{-form})_2Ir(OCOCF_3)_2(py)$ (**2**), has been isolated and characterized by X-ray crystallography: monoclinic, space group $P2_1/c$, a = 20.236 (6) Å, b = 10.151 (3) Å, c = 25.080 (11) Å, β = 96.02 (3)°, V = 5174 (3) Å^3, Z = 4, R = 0.0449, R_w = 0.0582 for 3796 data having $I > 3\sigma(I)$. A cyclic voltammetric study on compounds **1** and **2** is also reported.

Introduction

Rhodium(II) dimers containing four bidentate bridging ligands and a single metal–metal bond of $\sigma^2\pi^4\delta^2\delta^{*2}\pi^{*4}$ electronic configuration are well-known and relatively easily accessible in a number of ways,[1] the most common one being the direct interaction of $RhCl_3{\cdot}3H_2O$ with an alkali-metal salt of the desired bridging ligand in the presence of methanol, which is both the solvent and the reducing agent of the reaction. In such a way, simple compounds such as $Rh_2(OCOR)_4$ and $Rh_2(xhp)_4$ (xhp = 6-substituted hydroxypyridinato ion) have been prepared. On the other hand, the analogous Ir(II) compounds have not yet been reported, although a number of Ir(II) dimers with different structures are known, e.g. $[Ir(H)(\mu\text{-S-}t\text{-Bu})(CO)(P(OMe)_3)]_2$,[2] $Ir_2(C_{10}H_4S_4)Br_2(CO)_2(PPh_3)_2$,[3] $[IrX(\mu\text{-pz})(COD)]_2$ (X = Cl,[4]

(1) Cotton, F. A.; Walton, R. A. *Multiple Bonds Between Metal Atoms*; Wiley: New York, 1982.

(2) Bonnet, J. J.; Thorez, A.; Maisonnat, A.; Galy, J.; Poilblanc, R. *J. Am. Chem. Soc.* **1979**, *101*, 5940.

I[5]), $Ir_2I(CH_2I)(\mu\text{-pz})_2L_2$ [L = COD, $(CO)_2$, $(CO)(PPh_3)$][5] (pz = pyrazolato ion, COD = 1,5-cyclooctadiene), and $[Ir(\mu\text{-I})I(COD)]_2$.[6]

Recently the Ir(II) dimers $[Ir_2(TMB)_4I_2]^{2+}$ (TMB = 2,5-dimethyl-2,5-diisocyanohexane),[7] $Ir_2(Tcbiim)_2(CO)_2(MeCN)_2(P(OEt)_3)_2$ (Tcbiim = dianion of tetracyanobiimidazole),[8] and $[Ir(OEP)]_2$ (OEP = dianion of octaethylporphyrin)[9] have been reported, to which the $\sigma^2\pi^4\delta^2\delta^{*2}\pi^{*4}$ electronic configuration can be assigned. The first two of these have been structurally characterized and show Ir–Ir distances of 2.803[7] and 2.826 (2)[8] Å. It seems strange, therefore, that the simple Ir(II) carboxylates or any similar $Ir_2(LL)_4$ (LL = bidentate bridging monoanion) compounds have not yet been obtained, although efforts directed to such a goal have been made. For example, $[IrI_2(COD)]_2$ has been interacted with silver acetate,[6] but only the unusual $Ir_3(\mu_3\text{-O})_2(\mu\text{-I})(COD)_3$ cluster could be isolated in small yields after workup of the reaction mixture in the air.[6]

We decided to pursue the synthesis of Ir(II) dimers with four bidentate bridging anionic ligands and tried a new approach, based on the oxidation of Ir(I) dimers of the $[Ir(\mu\text{-LL})(COD)]_2$ type with agents capable of providing additional $(LL)^-$ ligands (e.g., PhCOO–OCOPh, $Tl(OCOCH_3)_3$, $AgOCOCF_3$, etc.). It is known, in fact, that Ir(I) dimers of that type undergo oxidative addition when they interact with molecules that generate monodentate anionic ligands, such as X_2 or XCH_2–X (X = halogen).[4-6]

While we investigated, with little success, a number of reactions of known Ir(I) dimers, we learned of the successful synthesis of $Rh_2(\mu\text{-form})_2(\mu\text{-OCOCF}_3)_2$ (form = *N,N'*-di-*p*-tolylformamidinato anion), isolated in a number of adducts with different axial ligands, by oxidation of $[Rh(\mu\text{-form})(COD)]_2$ with $AgOCOCF_3$.[10] We were then prompted to prepare the analogous Ir(I) compound, $[Ir(\mu\text{-form})(COD)]_2$,[11] and to study its reactivity toward oxidizing agents. We report here the results obtained with $AgOCOCF_3$, which differ somewhat from those of the corresponding rhodium system.

Experimental Section

Compound $[Ir(\mu\text{-form})(COD)]_2$ was prepared as previously described.[11] $AgOCOCF_3$ was purchased from Aldrich and used as received. Instruments used were as follows: IR, Perkin-Elmer 783; ^1H and ^{13}C NMR, Varian XL-200; CV, BAS-100. Elemental analyses were by Galbraith Laboratories, Knoxville, TN.

Reaction of $[Ir(\mu\text{-form})(COD)]_2$ with $AgOCOCF_3$. Preparation of $(COD)Ir(\mu\text{-form})_2Ir(OCOCF_3)_2(H_2O)\cdot C_6H_{14}$ (1). $[Ir(\mu\text{-form})(COD)]_2$ (0.60 g, 0.57 mmol) was stirred in 25 mL of commercial toluene (Fisher Scientific) at room temperature together with $AgOCOCF_3$ (0.26 g, 1.16 mmol). The reaction was conducted in air. A smooth reaction took place, consuming the partially undissolved Ir(I) starting material and giving rise to a yellow-brown solution and a gray solid. After overnight stirring, the solution was filtered through Celite and evaporated to dryness. The waxy residue was treated at room temperature with ca. 25 mL of *n*-hexane and the resulting mixture stirred for a few minutes. A microcrystalline dark precipitate formed. After overnight cooling at −20 °C, the solid was filtered off, washed with cold *n*-hexane, and dried in vacuo. Yield: 0.56 g (77%). Anal. Calcd for $C_{48}H_{58}F_6Ir_2N_4O_5$: C, 45.4; H, 4.6; N, 4.4. Found: C, 44.7; H, 4.6; N, 4.2. IR (Nujol mull; cm^{-1}): 1670 s, 1615 m, 1580 s, 1570 s, 1560 sh, 1510 sh, 1505 s, 1440 m, 1330 m, 1320 m–w, 1310 w, 1200 vs, 1160 w, 1150 s, 1115 w, 960 w, 945 w, 845 m–w, 820 m–w, 810 w, 790 w, 730 m, 555 w, 525 w. ^1H NMR (C_6D_6; δ): 9.40 (s, br, 2 H, H_2O); 7.46 (s, 2 H, N–C*H*–N); 7.20–6.75 (m, 16 H, $C_6H_4CH_3$); 5.34 (s, br, 2 H) and 4.07 (s, br, 2 H) (olef COD); 2.99 (s, br, 2 H) and 2.20–1.65 (m, 6 H) (aliph COD); 2.08 (s, 6 H) and 2.04 (s, 6 H) ($C_6H_4CH_3$); 1.23 (s, br, 8 H, CH_3–$(CH_2)_4$–CH_3); 0.89 (t, 6 H, CH_3–$(CH_2)_4$–CH_3). $^{13}C\{^1H\}$ NMR ($CDCl_3$; δ): 170.68 (q, $OCOCF_3$, J_{C-F} = 37.3 Hz); 165.03 (N–*C*H–N); 145.98, 145.85, 135.75, and 135.29 (ipso + para $C_6H_4CH_3$); 129.61, 129.46, 126.69, and 125.77 (ortho + meta $C_6H_4CH_3$); 114.90 (q, $OCOCF_3$, J_{C-F} = 289.3 Hz); 89.07 and 85.56 (olef COD); 32.56 and 29.28 (aliph COD); 31.62 and 22.69 (CH_3–$(CH_2)_4$–CH_3); 21.09 and 20.80 ($C_6H_4CH_3$); 14.16 (CH_3–$(CH_2)_4$–CH_3). Compound **1** dissolves in toluene, THF, CH_2Cl_2, and hot *n*-hexane to afford dichroic green–red solutions that are stable in air for at least several days.

Treatment of 1 with Pyridine. The reaction of **1** with pyridine was first tested in the NMR tube (see Results and Discussion): a sample of **1** dissolved in C_6D_6 under argon was treated with a few drops (excess) of pyridine-d_5. The color immediately changed to dark red, and the ^1H NMR spectrum had the following peaks (δ): 8.55 (s, br, 2 H); 7.83 (s, 2 H); 7.5–6.8 (m, 16 H); 5.40 (s, br, 2 H); 4.21 (s, br, 2 H); 3.26 (s, br, 2 H); 2.07 (s, 6 H); 1.95 (s, 6 H); 2.0–1.5 (m, 6 H); 1.21 (s, br, 8 H); 0.87 (t, 6 H).

A concentrated solution of **1** was treated with an excess of pyridine and then layered with *n*-hexane. Slow diffusion produced dark red crystals and an orange powder. One of the red crystals (compound **2**) was subjected to an X-ray crystallographic study.

X-ray Crystallography for Compound 2. Data collection and reduction were routine. Axial photographs and systematic absences from the data uniquely determined the space group as the monoclinic $P2_1/c$. The structure was solved by standard Patterson methods and refined by subsequent cycles of full-matrix least squares and difference Fourier maps. The Enraf-Nonius SDP software was employed on PDP/11 and VAX computers. At the end of the isotropic refinement on the diiridium molecule an absorption correction was applied according to the method of Walker and Stuart.[12] Subsequent anisotropic refinement led to convergence at R = 0.063. At this point a number of peaks of ca. 1.5 e $Å^{-3}$ were still present in the difference Fourier map in a region of space

Table I. Crystal Data for Compound **1**

formula	$C_{53}H_{61}F_6Ir_2N_5O_4$
formula weight	1283.12
space group	$P2_1/c$
systematic absences	$h0l$, $l \neq 2n$; $0k0$, $k \neq 2n$
a, Å	20.236 (6)
b, Å	10.251 (3)
c, Å	25.080 (11)
α, deg	90
β, deg	96.02 (3)
γ, deg	90
V, $Å^3$	5174 (3)
Z	4
d_{calcd}, g/cm^3	1.647
crystal size, mm	0.25 × 0.30 × 0.50
μ(Mo Kα), cm^{-1}	51.851
data collcn instrument	Syntex P3
radiation (monochromated in incident beam)	Mo Kα (λ_α = 0.71073 Å)
orientation reflcns: no.; range (2θ), deg	25; 20–25
temp, °C	25
scan method	ω
data collcn range (2θ), deg	4–45
no. of unique data; total with $F_o^2 > 3\sigma(F_o^2)$	4712; 3796
no. of params refined	572
trans factors: max; min	1.0; 0.29
R^a	0.0449
R_w^b	0.0582
quality-of-fit indicator[c]	1.139
largest shift/esd, final cycle	0.36
largest peak, e/$Å^3$	0.921

[a] $R = \sum||F_o| - |F_c||/\sum|F_o|$. [b] $R_w = [\sum w(|F_o| - |F_c|)^2/\sum w|F_o|^2]^{1/2}$; $w = 1/\sigma^2(|F_o|)$. [c] Quality-of-fit = $[\sum w(|F_o| - |F_c|)^2/(N_{observns} - N_{params})]^{1/2}$.

(3) Teo, B.-K.; Snyder-Robinson, P. A. *J. Chem. Soc., Chem. Commun.* **1979**, 255.
(4) (a) Caspar, J. V.; Gray, H. B. *J. Am. Chem. Soc.* **1984**, *106*, 3029. (b) Marshall, J. L.; Stobart, S. R.; Gray, H. B. *J. Am. Chem. Soc.* **1984**, *106*, 3027.
(5) Harrison, D. G.; Stobart, S. R. *J. Chem. Soc., Chem. Commun.* **1986**, 285.
(6) Cotton, F. A.; Lahuerta, P.; Sanau, M.; Schwotzer, W. *J. Am. Chem. Soc.* **1985**, *107*, 8284.
(7) Miskowski, V. M.; Smith, T. P.; Loehr, T. M.; Gray, H. B. *J. Am. Chem. Soc.* **1985**, *107*, 7925.
(8) Rasmussen, P. G.; Anderson, J. E.; Bailey, O. H.; Tamres, M. *J. Am. Chem. Soc.* **1985**, *107*, 279.
(9) Del Rossi, K. J.; Wayland, B. B. *Abstracts of Papers*, 192nd National Meeting of the American Chemical Society, Anaheim, CA; American Chemical Society: Washington, DC, 1986; INOR 344.
(10) Piraino, P.; Bruno, G.; Tresoldi, G.; Lo Schiavo, S.; Zanello, P. *Inorg. Chem.*, in press.
(11) Cotton, F. A.; Poli, R. *Inorg. Chim. Acta* **1986**, *122*, 243.
(12) Walker, N.; Stuart, D. *Acta Crystallogr., Sect. A: Found. Crystallogr.* **1983**, *A39*, 158.

Table II. Atomic Positional Parameters and Equivalent Isotropic Displacement Parameters and Their Estimated Standard Deviations for $(COD)Ir(\mu\text{-form})_2Ir(OCOCF_3)_2(py)\cdot C_6H_{14}$[a]

atom	x	y	z	B, Å²
Ir1	0.84615 (3)	−0.04004 (7)	0.70706 (2)	2.63 (1)
Ir2	0.78858 (3)	−0.04862 (7)	0.80264 (2)	2.54 (1)
F1	0.9697 (7)	0.077 (2)	0.9203 (7)	16.9 (5)
F2	0.9226 (7)	0.215 (2)	0.9641 (4)	15.5 (6)
F3	0.9545 (7)	0.260 (2)	0.8966 (6)	12.9 (5)
F4	0.7400 (7)	0.389 (1)	0.7862 (7)	12.0 (5)
F5	0.6562 (9)	0.345 (1)	0.8186 (6)	20.7 (6)
F6	0.6544 (9)	0.380 (2)	0.7436 (7)	16.8 (6)
O1	0.8661 (5)	0.038 (1)	0.8525 (3)	3.2 (2)
O2	0.8124 (6)	0.178 (1)	0.9029 (4)	6.2 (3)
O3	0.7494 (5)	0.140 (1)	0.7926 (4)	3.3 (2)
O4	0.6467 (6)	0.127 (1)	0.7462 (5)	6.7 (3)
N1	0.8432 (5)	−0.233 (1)	0.7192 (4)	2.1 (2)*
N2	0.8367 (6)	−0.224 (1)	0.8110 (4)	2.8 (3)
N3	0.7486 (5)	−0.052 (1)	0.6749 (4)	3.0 (3)
N4	0.7119 (5)	−0.137 (1)	0.7540 (4)	2.3 (3)
N5	0.7358 (6)	−0.061 (1)	0.8693 (4)	3.6 (3)
C1	0.8474 (7)	−0.291 (2)	0.7690 (5)	3.7 (4)
C2	0.7034 (8)	−0.110 (2)	0.7013 (5)	3.5 (4)
C3	0.8596 (8)	0.121 (2)	0.8892 (6)	4.5 (4)
C4	0.925 (1)	0.162 (2)	0.9189 (7)	7.8 (7)
C5	0.6969 (8)	0.178 (2)	0.7720 (6)	4.0 (4)
C6	0.6885 (9)	0.324 (2)	0.7767 (8)	5.1 (5)
C10	0.8347 (8)	−0.328 (1)	0.6769 (6)	3.7 (4)
C11	0.790 (1)	−0.430 (2)	0.6780 (6)	5.0 (5)
C12	0.782 (1)	−0.522 (2)	0.6359 (7)	6.4 (6)
C13	0.825 (1)	−0.510 (2)	0.5935 (6)	5.8 (5)
C14	0.8634 (9)	−0.402 (2)	0.5903 (6)	4.6 (4)
C15	0.8691 (9)	−0.309 (2)	0.6322 (6)	4.7 (5)
C16	0.815 (1)	−0.617 (2)	0.5476 (7)	8.0 (6)
C20	0.8599 (7)	−0.294 (2)	0.8617 (5)	3.3 (4)
C21	0.8340 (7)	−0.411 (2)	0.8749 (6)	3.2 (4)
C22	0.8537 (8)	−0.468 (2)	0.9244 (6)	4.3 (4)
C23	0.9012 (8)	−0.405 (2)	0.9607 (6)	4.3 (4)
C24	0.9295 (8)	−0.287 (2)	0.9462 (6)	3.9 (4)
C25	0.9095 (8)	−0.229 (2)	0.8949 (6)	3.9 (4)
C26	0.919 (1)	−0.466 (2)	1.0172 (7)	6.6 (5)
C30	0.7260 (7)	−0.002 (2)	0.6229 (6)	3.3 (4)
C31	0.6826 (9)	0.096 (2)	0.6165 (6)	4.8 (5)
C32	0.664 (1)	0.146 (2)	0.5645 (7)	7.1 (6)
C33	0.6891 (9)	0.094 (2)	0.5206 (7)	5.8 (5)
C34	0.7324 (9)	−0.015 (2)	0.5286 (7)	5.7 (5)
C35	0.7517 (9)	−0.063 (2)	0.5792 (6)	5.2 (5)
C36	0.670 (1)	0.147 (3)	0.4619 (8)	9.9 (8)
C40	0.6596 (7)	−0.203 (2)	0.7753 (6)	3.1 (4)
C41	0.5937 (8)	−0.160 (2)	0.7592 (6)	4.5 (5)
C42	0.5419 (8)	−0.224 (2)	0.7824 (7)	6.5 (6)
C43	0.5563 (8)	−0.323 (2)	0.8210 (6)	4.9 (5)
C44	0.6208 (8)	−0.359 (2)	0.8370 (6)	5.0 (5)
C45	0.6731 (8)	−0.303 (2)	0.8119 (6)	4.1 (4)
C46	0.496 (1)	−0.394 (3)	0.8455 (9)	9.4 (7)
C51	0.6726 (8)	−0.018 (2)	0.8651 (7)	4.3 (4)
C52	0.6337 (9)	−0.023 (2)	0.9084 (7)	6.5 (5)
C53	0.664 (1)	−0.073 (2)	0.9605 (9)	7.9 (7)
C54	0.729 (1)	−0.116 (2)	0.9607 (6)	5.7 (5)
C55	0.7650 (9)	−0.107 (2)	0.9175 (6)	4.7 (4)
C60	0.9530 (7)	−0.065 (2)	0.7089 (6)	3.4 (4)
C61	0.9405 (7)	−0.005 (2)	0.7563 (6)	3.2 (4)
C62	0.9537 (9)	0.141 (2)	0.7692 (6)	4.7 (4)
C63	0.8903 (8)	0.226 (2)	0.7554 (6)	4.1 (4)
C64	0.8424 (7)	0.177 (1)	0.7103 (6)	3.0 (4)
C65	0.8663 (8)	0.130 (2)	0.6621 (7)	3.8 (4)
C66	0.9382 (9)	0.141 (2)	0.6484 (7)	4.7 (4)
C67	0.9762 (8)	0.011 (2)	0.6611 (6)	3.7 (4)

[a] Starred value indicates atom was refined isotropically. Anisotropically refined atoms are given in the form of the equivalent isotropic displacement parameter defined as $^4/_3[a^2\beta_{11} + b^2\beta_{22} + c^2\beta_{33} + ab(\cos\gamma)\beta_{12} + ac(\cos\beta)\beta_{13} + bc(\cos\alpha)\beta_{23}]$.

away from the diiridium molecule. These indicated the presence of solvent of crystallization. The eight most intense peaks were included in the atom list as full-occupancy carbon atoms and refined, but a clear picture of a solvent molecule did not emerge. The possibility of disorder was also considered, but an attempt to refine the occupancy factors, while holding the isotropic thermal parameters U fixed at the reasonable value of 0.15 Å² for these atoms, did not improve the quality of the model. We concluded that we presumably have a badly disordered solvent molecule, most probably hexane (see Results and Discussion), and we left the eight previously mentioned peaks in the final cycles of refinement on the ground that convergence is achieved at a lower final agreement factor ($R = 0.0449$; $R_w = 0.0582$), thus affording a chemically more significant picture of the diiridium molecule. The N1 atom refined with a non positive definite thermal tensor, and it was therefore left isotropic in the last cycles of refinement.

Table III. Selected Bond Distances (Å) and Angles (deg) and Their Estimated Standard Deviations for $(COD)Ir(\mu\text{-form})_2Ir(OCOCF_3)_2(py)\cdot C_6H_{14}$[a]

Ir1–Ir2	2.774 (1)	O2–C3	1.20 (2)
Ir1–N1	2.003 (12)	O3–C5	1.20 (2)
Ir1–N3	2.055 (11)	O4–C5	1.26 (2)
Ir1–C60	2.174 (13)	N1–C1	1.38 (2)
Ir1–C61	2.191 (14)	N1–C10	1.44 (2)
Ir1–C64	2.226 (15)	N2–C1	1.29 (2)
Ir1–C65	2.14 (2)	N2–C20	1.49 (2)
Ir2–O1	2.097 (10)	N3–C2	1.33 (2)
Ir2–O3	2.093 (11)	N3–C30	1.43 (2)
Ir2–N2	2.049 (12)	N4–C2	1.35 (2)
Ir2–N4	2.081 (11)	N4–C40	1.40 (2)
Ir2–N5	2.081 (11)	C60–C61	1.39 (2)
O1–C3	1.27 (2)	C64–C65	1.43 (2)
Ir2–Ir1–N1	79.3 (3)	O1–Ir2–N5	87.8 (4)
Ir2–Ir1–N3	82.2 (3)	O3–Ir2–N2	173.8 (4)
Ir2–Ir1–C60	119.0 (4)	O3–Ir2–N4	94.8 (5)
Ir2–Ir1–C61	86.5 (4)	O3–Ir2–N5	86.0 (5)
Ir2–Ir1–C64	88.9 (4)	N2–Ir2–N4	89.6 (5)
Ir2–Ir1–C65	127.1 (5)	N2–Ir2–N5	98.3 (5)
N1–Ir1–N3	87.8 (5)	N4–Ir2–N5	91.8 (5)
N1–Ir1–C60	85.6 (6)	Ir2–O1–C3	126 (1)
N1–Ir1–C61	96.6 (5)	Ir2–O3–C5	131 (1)
N1–Ir1–C64	168.1 (5)	Ir1–N1–C1	125 (1)
N1–Ir1–C65	153.5 (6)	Ir1–N1–C10	124 (1)
N3–Ir1–C60	156.0 (5)	C1–N1–C10	112 (1)
N3–Ir1–C61	166.9 (5)	Ir2–N2–C1	120 (1)
N3–Ir1–C64	92.1 (5)	Ir2–N2–C20	127.8 (9)
N3–Ir1–C65	93.9 (6)	C1–N2–C20	112 (1)
C60–Ir1–C61	37.1 (5)	Ir1–N3–C2	121 (1)
C60–Ir1–C64	99.0 (6)	Ir1–N3–C30	122.7 (9)
C60–Ir1–C65	82.2 (6)	C2–N3–C30	116 (1)
C61–Ir1–C64	81.1 (6)	Ir2–N4–C2	120 (1)
C61–Ir1–C65	87.7 (6)	Ir2–N4–C40	122.1 (9)
C64–Ir1–C65	38.3 (6)	C2–N4–C40	117 (1)
Ir1–Ir2–O1	98.4 (3)	N1–C1–N2	120 (2)
Ir1–Ir2–O3	93.2 (3)	N3–C2–N4	124 (1)
Ir1–Ir2–N2	83.0 (3)	O1–C3–O2	133 (2)
Ir1–Ir2–N4	82.1 (3)	O3–C5–O4	136 (2)
Ir1–Ir2–N5	173.7 (4)	Ir1–C60–C61	72.2 (8)
O1–Ir2–O3	86.1 (4)	Ir1–C61–C60	70.8 (8)
O1–Ir2–N2	89.6 (5)	Ir1–C64–C65	67.4 (9)
O1–Ir2–N4	179.0 (4)	Ir1–C65–C64	74.3 (9)

[a] Numbers in parentheses are estimated standard deviations in the least significant digits.

Significant crystal data are reported in Table I. Table II contains the fractional atomic coordinates and equivalent isotropic thermal parameters of the atoms in the diiridium molecule, while relevant bond distances and angles are listed in Table III. The coordinates of the peaks assigned to the disordered solvent molecule are given in the supplementary material, together with the anisotropic thermal parameters of all atoms, full tables of bond distances and angles, and a listing of the observed and calculated structure factors.

Results and Discussion

A preliminary electrochemical investigation was carried out on the compounds $[Ir(\mu\text{-LL})(COD)]_2$ (LL = form,[11] hp[13]). The cyclic voltammogram for each compound in THF with tetra-*n*-butylammonium hexafluorophosphate as supporting electrolyte exhibits a quasi-reversible oxidation process. The half-wave potential for the hydroxypyridinato compound is +0.686 V vs.

(13) Rodman, G. S.; Mann, K. R. *Inorg. Chem.* **1985**, *24*, 3507.

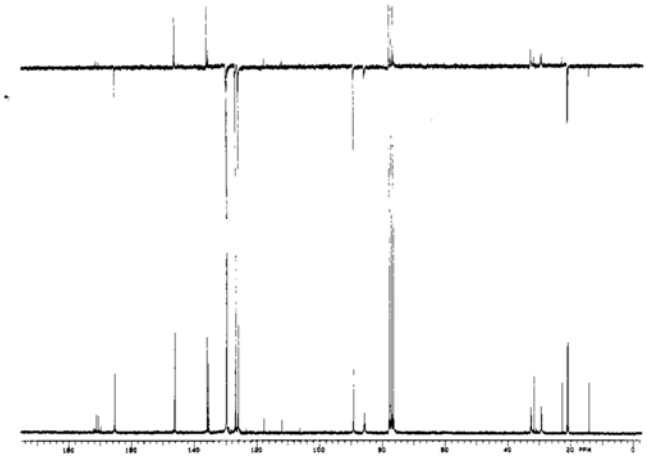

Figure 1. ^{13}C NMR spectra of compound **1**: (bottom) $^{13}C\{^1H\}$ NMR spectrum; (top) $^{13}C\{APT\}$ NMR spectrum. Solvent = $CDCl_3$; T = 25 °C.

aqueous Ag/AgCl (ΔE_p = 324 mV at a scan rate of 100 mV s^{-1}; ΔE_p = 198 mV at 20 mV s^{-1}). The oxidation process for the formamidine derivative appears at a less positive potential ($E_{1/2}$ = 0.515 V), and it is more reversible (ΔE_p = 153 mV at 100 mV s^{-1}; 104 mV at 15 mV s^{-1}). Compounds $[Ir(\mu\text{-mhp})(COD)]_2$ (mhp = 6-methylhydroxypyridinato ion) and $[Ir(\mu\text{-pz})(COD)]_2$ were also found to undergo a quasi-reversible oxidation process.[13] This result shows that the formamidinato derivative is a better candidate for chemical oxidation reactions.

Synthesis and Spectroscopic Characterization. The reaction of $[Ir(\mu\text{-form})(COD)]_2$ with 2 equiv of $AgOCOCF_3$ was first carried out under exclusion of air and by using dry solvents. Oxidation took place, as evidenced by the formation of metallic silver. Subsequent workup of the mixture led, however, to the isolation of a crystalline material in very low yields. A thorough spectroscopic study, and further evidence from the crystal structure determination of the pyridine derivative (vide infra), allowed the identification of the product as $(COD)Ir(\mu\text{-form})_2Ir(OCOCF_3)_2(H_2O)\cdot n\text{-}C_6H_{14}$ (**1**). The water ligand may have been

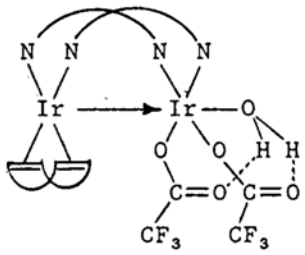

1

obtained from the silver salt reagent (which is hygroscopic) or from incompletely dried Celite or glassware. At any rate, once the structure and the stability to air of the product had been established, the synthesis was optimized to ca. 80% isolated yields by simply working in air and using commercial undistilled solvents.

The ^1H and $^{13}C\{^1H\}$ NMR techniques, the latter in conjunction with an attached proton test (APT),[14] proved to be very powerful tools for establishing the structure of compound **1**. The $^{13}C\{^1H\}$ and $^{13}C\{APT\}$ NMR spectra of compound **1** are reported in Figure 1.

The formamidinato ligands exhibit only one type of formamidine functionality (proton singlet at δ 7.46, carbon singlet at δ 165.03) but two types of *p*-tolyl groups (proton, two singlets at δ 2.08 and 2.04 for the methyl groups; carbon, two singlets at δ 21.09 and 20.80 for the methyl groups and two singlets for each of the four different ring carbons, i.e. ipso, ortho, meta, and para), indicating that one or more equivalent formamidinato ligands bridge two nonequivalent metals. A full assignment of the signals due to the ring carbon atoms is not possible on the basis of the experiments performed. However, the $^{13}C\{APT\}$ NMR spectrum indicates that the peaks at δ 145.98, 145.85, 135.75, and 135.29 correspond to ipso and para carbon atoms (peaks up, even number of attached protons) and those at δ 129.61, 129.46, 126.69, and 125.77 are due to the ortho and meta carbon atoms (peaks down, odd number of attached protons). The COD ligand exhibits two different types of olefin protons (assigned to the endo and exo positions) at δ 5.34 and 4.07 and, accordingly, two types of olefin carbon atoms at δ 89.07 and 85.56. The aliphatic protons of the COD ligand give rise to a complicated pattern, but the corresponding methylene carbon atoms again give rise to two peaks at δ 32.56 and 29.28 for the endo and exo positions. Integration of the proton spectrum establishes that there are two formamidinato groups per COD ligand.

The trifluoroacetato groups (two per dimer by elemental analyses) are equivalent, since only one quartet is present for the trifluoromethyl carbon atom at δ 114.90 (J_{C-F} = 289.3 Hz) and another one for the carboxylic carbon atom at δ 170.68 (J_{C-F} = 37.3 Hz). The $^{13}C\{^1H\}$ NMR spectrum shows three more peaks at δ 31.62, 22.69 and 14.16 ppm. These can be attributed to *n*-hexane present in the lattice. This is consistent with the following observations: (i) the ^1H NMR spectrum shows the corresponding proton peaks at δ 1.23 (broad singlet) and 0.89 (triplet), consistent with a dimer/hexane ratio of 1; (ii) the $^{13}C\{APT\}$ NMR spectrum indicates the peak at δ 14.16 to be due to the methyl groups and the other two to the methylene groups; (iii) the elemental analysis of compound **1** gives good agreement only with the calculated values for the structure with one hexane molecule of crystallization per dimer; and, finally, (iv) the workup of compound **1** described in the Experimental Section shows that hexane is necessary in order to obtain a crystalline material.

A peak in the proton spectrum at δ 9.40 still remains to be accounted for. This corresponds to two protons per dimeric unit. These protons are assigned to a water molecule which, as indicated by the unusually low field chemical shift, must be strongly hydrogen bonded. The structure illustrated for compound **1** almost directly follows. The presence of water is supported by elemental analyses, by the increased yields obtained when wet solvents are used, and by the displacement reactions described below.

The reactions of **1** in C_6D_6 at room temperature with an excess of each of the deuteriated donor ligands pyridine, dimethyl sulfoxide (Me_2SO), and acetonitrile (eq 1) were followed by ^1H NMR spectroscopy.

$$\underset{\mathbf{1}}{(COD)Ir(\mu\text{-form})_2Ir(OCOCF_3)_2(H_2O)} + L \rightleftharpoons (COD)Ir(\mu\text{-form})_2Ir(OCOCF_3)_2L + H_2O \quad (1)$$

L: py-d_5, **2**; Me_2SO-d_6, **3**; (Me-d_3)CN, **4**

The color changed rapidly to dark red (py) or orange (Me_2SO and MeCN). The ^1H NMR spectra of the resulting mixtures showed, as the principal features, a decrease in intensity of the peak assigned to coordinated water and, in two cases, the appearance of another peak at a position that depends on the added ligand. This new peak was at δ 3.38 for L = Me_2SO and 1.61 for L = MeCN. We assign these peaks to free water formed according to eq 1, and we attribute the differences in chemical shift observed in the different experiments to the different degrees of hydrogen bonding of the free water with the excess of added donor ligand L, in the order Me_2SO > MeCN. No new peak appeared when L = py that could be assigned to water. This is presumably because of fast hydrogen exchange on the NMR time scale caused by the excess of pyridine. The reaction was complete for L = py, as indicated by the disappearance of the coordinated water peak in the ^1H NMR spectrum, while in the other two cases an equilibrium was reached. Because of the difficulty in calibrating the amount of added L, however, a value for the equilibrium constant could not be obtained.

We can envisage the formation of **1** from $[Ir(\mu\text{-form})(COD)]_2$ and $AgOCOCF_3$ as resulting from a double-electron oxidation

(14) (a) Rabenstein, D. L.; Nakachima, T. T. *Anal. Chem.* **1979**, *51*, 1465A. (b) Lecocq, C.; Lallemand, J.-Y. *J. Chem. Soc., Chem. Commun.* **1981**, 150. (c) Patt, S. L.; Shoolery, J. N. *J. Magn. Reson.* **1982**, *46*, 535.

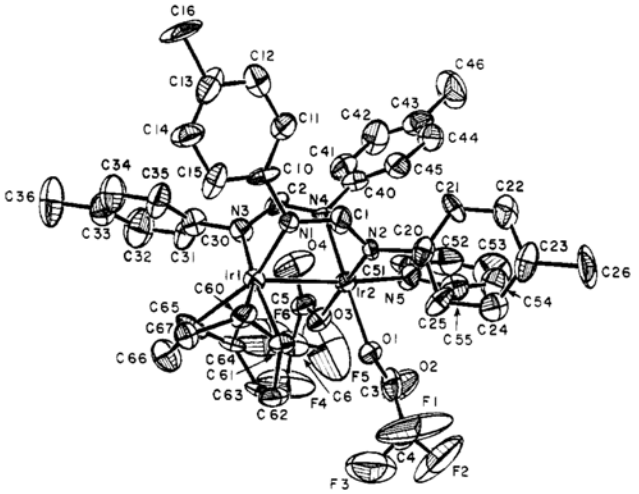

Figure 2. ORTEP view of compound **2** with the atomic numbering scheme employed.

Scheme I

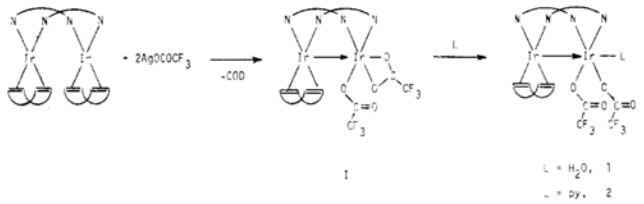

at one iridium center with expulsion of COD and coordination of the two trifluoroacetato groups. The intermediate I depicted in Scheme I would presumably be the final product in strictly anhydrous conditions. This product presumably interacts very easily with donor molecules, according to Scheme I.

When L = H_2O, the final product acquires particular stability because of the formation of two six-membered rings containing hydrogen-bonding interactions between the water hydrogen atoms and the trifluoroacetato carbonyl oxygen atoms. In fact, compound **1** can be recovered unaltered (by ^1H NMR) after short reflux in C_6D_6, whereas compound **2** rapidly decomposes.

Compound **1** was also obtained in good yields when the oxidation reaction was carried out in THF as solvent. In this case another intermediate, containing THF as axial ligand, might be formed. The isolation from this reaction mixture of the H_2O adduct and not of the THF adduct again suggests the higher stability of the hydrogen-bonded structure of compound **1**.

Crystal Structure of Compound 2. The derivative obtained from compound **1** by displacing H_2O with pyridine (compound **2**) was isolated in the form of single crystals and subjected to an X-ray crystallographic study. It consists of discrete molecules of $(COD)Ir(\mu\text{-form})_2Ir(OCOCF_3)_2(py)$ that occupy a general position. A view of the molecule is shown in Figure 2. The crystal structure also shows one disordered solvent of crystallization molecule per dimer. The identity of this solvent molecule could not be unequivocally established by crystallography; by analogy with compound **1** we suggest this to be *n*-hexane.

The coordination geometry around Ir1 is square planar, the coordination positions being occupied by two nitrogen atoms of the bridging formamidinato groups and by the two olefinic functionalities of the cyclooctadiene ligand. It may also be considered to be square pyramidal, the Ir2 atom occupying the apical position; the square-planar picture, however, agrees better with the electronic description of the molecule (vide infra). The coordination around Ir2 is, on the other hand, octahedral, with two formamidinato nitrogen atoms and two trifluoroacetato oxygen atoms in a square plane, and Ir1 and the pyridine ligand occupying the remaining axial positions.

The average oxidation state for iridium is II, but the description of the dimer as a mixed-valence Ir(I)–Ir(III) compound seems more suitable, since the square-planar configuration found around

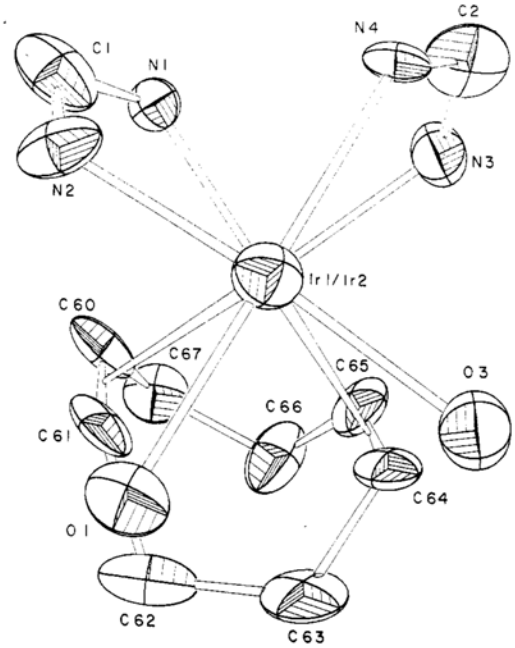

Figure 3. Central portion of the molecule of compound **2** viewed along the Ir1–Ir2 vector.

Ir1 is typical for d^8 Ir(I), while d^6 Ir(III) prefers a closed-shell octahedral configuration, like that found around Ir2. Ir1 is therefore acting as a donor ligand, providing two electrons to complete the coordination sphere of Ir2 through its d_{z^2} orbital. The metal–metal interaction (Ir1–Ir2: 2.774 (1) Å) can therefore be best viewed as a dative Ir(I)→Ir(III) bond. The alternative description as a homogeneous-valence Ir(II) dimer, in which we account for the presence of a metal–metal interaction through a covalent single bond, is less plausible because of the markedly different coordination shells of the two Ir atoms, but it cannot be ruled out apodictically. This is, to the best of our knowledge, the first reported example of a dative Ir(I)→Ir(III) bond, although several examples of other homonuclear and heteronuclear dative metal–metal bonds are known.[15]

The least-squares equatorial planes around the two metal atoms form a dihedral angle, θ, of 26.7° (deviations of the iridium atoms from the corresponding planes are 0.108 (1) Å for Ir1 and 0.035 (1) Å for Ir2). The two equatorial square planes are twisted around the Ir1–Ir2 vector, as shown by the projection of Figure 3. The average twist angle is 23.3 (5)°. These two features are probably the result of the competing effects of three factors: the metal–metal interaction, the steric repulsion between the cyclooctadiene ligand and the trifluoroacetato groups, and the "bite" distance required by the two bridging formamidinato ligands. It is not difficult to visualize that a rotation around the Ir1–Ir2 vector to obtain the eclipsed conformation would cause the angle θ to decrease if the N1···N2, N3···N4, and Ir1–Ir2 distances are to be left unchanged. This would cause the COD and the trifluoroacetato groups to come closer to each other. There is a tendency, therefore, to alleviate this van der Waals repulsion by twisting and bending. No particular stress seems to be present on the formamidinato groups, since the N–C(H) distances (average 1.34 (2) Å) and the N–C–N angles (average 122 (2)°) are within the normal range for this type of bond. In particular they are similar to those found in $Rh_2(form)_2(OCOCF_3)_2(H_2O)_2$ (C–N

(15) (a) Barr, R. D.; Marder, T. B.; Orpen, A. G.; Williams, I. D. *J. Chem. Soc., Chem. Commun.* **1984**, 112. (b) Fleming, M. M.; Pomeroy, R. K.; Rushman, P. *J. Organomet. Chem.* **1984**, *273*, C33. (c) Einstein, F. W. B.; Martin, L. R.; Pomeroy, R. K.; Rushman, P. *J. Chem. Soc., Chem. Commun.* **1985**, 345. (d) Targos, T. S.; Rosen, R. P.; Whittle, R. R.; Geoffroy, G. L. *Inorg. Chem.* **1985**, *24*, 1375. (e) Baker, R. T.; Tulip, T. H.; Wreford, S. S. *Inorg. Chem.* **1985**, *24*, 1379. (f) Mercer, W. C.; Whittle, R. R.; Burkhardt, E. W.; Geoffroy, G. L. *Organometallics* **1985**, *4*, 68. (g) Einstein, F. W. B.; Pomeroy, R. K.; Rushman, P.; Willis, A. C. *Organometallics* **1985**, *4*, 250.

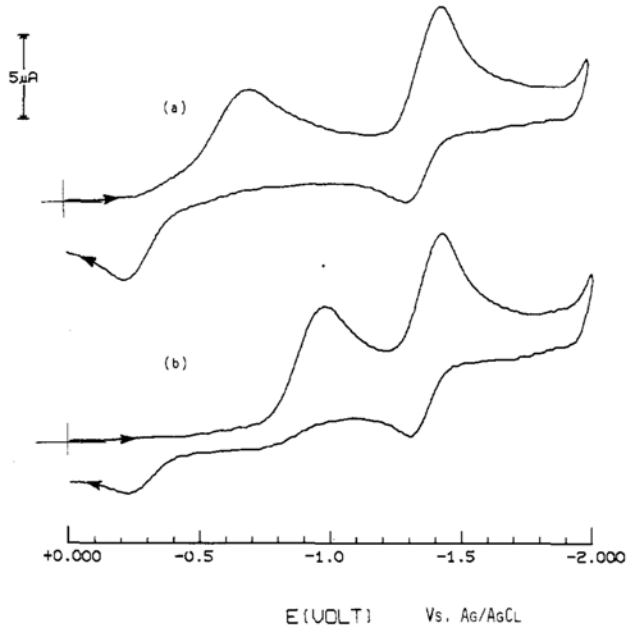

Figure 4. Cyclic voltammograms of $(COD)Ir(\mu\text{-form})_2Ir(OCOCF_3)_2(L)$ in THF (0.1 M n-Bu_4PF_6) at a glassy carbon electrode: (a) L = H_2O; (b) L = pyridine. The solution of compound **2** used for recording voltammogram b has been obtained in situ by adding a small excess (a few drops) of pyridine to the solution of compound **1** previously used for recording voltammogram a. Scan rate = 100 mV s^{-1}; T = 25 °C.

= 1.308 (6) Å, N–C–N = 124.6 (4)°, average values).[10] This situation differs from that present in formamidinato derivatives of quadruply bonded dimers. In such cases the shorter metal–metal separation and the presence of the δ bond, which contributes an additional barrier to internal rotation around the metal–metal vector, cause some stress to be put on the formamidinato bridges, as evidenced by the lower N–C–N angles [116 (2)° in monoclinic $Re_2(N_2CPh_3)_2Cl_4$ and 117 (2)° (average) in triclinic $Re_2(N_2CPh_3)_2Cl_4(THF)$,[16] 117 (1)° (average) in $Mo_2(N_2CPh_3)_4$,[17] and 116.4 (5)° (average) in $Cr_2(MeNCPhNMe)_4$[18]].

The Ir2–N5 distance of 2.08 (1) Å is very similar to the other Ir–N distances of the molecule, thus indicating no particular trans influence of the Ir(I)-based donor ligand.

Cyclic Voltammetry Study. Compounds **1** and **2** do not exhibit any significant oxidation wave up to a potential where electrolysis of the solvent (THF) becomes appreciable (ca. +0.8 V vs. aqueous Ag/AgCl). On the other hand, they undergo interesting reduction processes. Figure 4a shows the cyclic voltammogram of compound **1**. This exhibits a first reduction wave with E_p = ca. −0.70 V and a second one with E_p = ca. −1.44 V. The second process is quasi-reversible (ΔE_p = 127 mV at a scan rate of 100 mV s^{-1}, $E_{1/2}$ = −1.37 V), while the reverse wave related to the first reduction process is shifted to a much more positive potential (E_p = ca. −0.24 V), indicating that a coupled chemical reaction is presumably taking place.

The cyclic voltammogram, recorded under the same conditions, of compound **2**, shown in Figure 4b, confirms this hypothesis and suggests a possible mechanism for the whole electrochemical process. The first reduction wave is shifted from the corresponding one of compound **1** to a more negative potential (E_p = ca. −0.98 V) while all the rest of the voltammogram remains unchanged within the experimental error. This indicates that the same couple is responsible for the process at −1.37 V in both cases. Fast loss of the axial ligand from the octahedrally coordinated iridium is therefore suggested after the first reduction process has taken place. The mechanism illustrated in Scheme II emerges. The electrochemically generated Ir(I)–Ir(II) species contains a 19e Ir(II) center. This would then rapidly lose its axial ligand to afford a species that is common to the two voltammograms. This would then give rise to a second reduction wave at more negative potentials, presumably to produce an Ir(I)–Ir(I) dianion, while at more positive potentials it generates an oxidation wave to produce a new Ir(I)–Ir(III) species where Ir(III) is void of axial ligand and has 16 electrons in its valence shell. Such a species readily reacts with the ligand L to restore compound **1** or **2**; this is indicated by the observation that subsequent scans do not show any change in the voltammograms with respect to those of Figure 4.

Scheme II

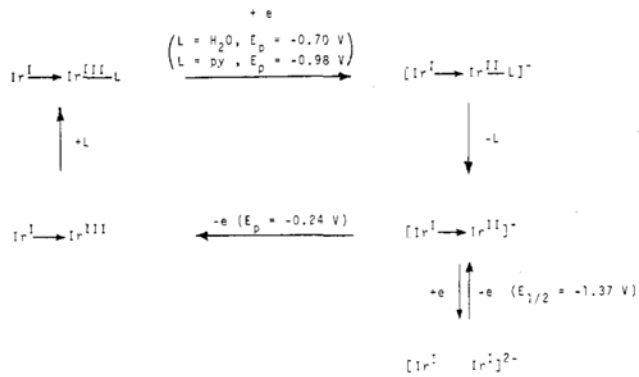

Conclusions

Oxidation of $[Ir(\mu\text{-form})(COD)]_2$ with $AgOCOCF_3$ affords mixed-valence Ir(I)–Ir(III) compounds containing a dative metal–metal bond.

It is interesting to compare our results with those obtained by Piraino et al. on the analogous rhodium system.[10] The reaction between $[Rh(\mu\text{-form})(COD)]_2$ and $AgOCOCF_3$ was reported to lead to the formation of homogeneous-valence Rh(II) dimers. No evidence of the formation of Rh(I)–Rh(III) systems similar to the Ir compounds described in this paper was reported. It can be seen that the mixed-valence structure could be formally converted into the homogeneous-valence one by simply removing the residual COD ligand on Ir(I) and converting the two monodentate trifluoroacetato groups to bidentate bridging ligands. This should of course be accompanied by an electron redistribution among the metal atoms.

It is not impossible that the mixed-valence structure is an actual intermediate in the rhodium reaction, whereas when the metal is iridium, such a structure is presumably thermodynamically more stable and can be therefore isolated. Efforts to convert these mixed-valence Ir dimers to the still elusive quadruply bridged Ir(II) dimers are currently under way in this laboratory.

Acknowledgment. We are indebted to Professor P. Piraino for sending us a copy of his manuscript[10] prior to publication. We also thank the NSF for support of this work.

Supplementary Material Available: Tables of fractional coordinates of the disordered solvent molecule and anisotropic displacement parameters and full tables of bond lengths and angles (7 pages); a listing of observed and calculated structure factors (19 pages). Ordering information is given on any current masthead page.

(16) Cotton, F. A.; Shive, L. W. *Inorg. Chem.* **1975**, *14*, 2027.
(17) Cotton, F. A.; Inglis, T.; Kilner, M.; Webb, T. R. *Inorg. Chem.* **1975**, *14*, 2023.
(18) Bino, A.; Cotton, F. A.; Kaim, W. *Inorg. Chem.* **1979**, *18*, 3566.